Wong *et al. Fire Ecology* (2025) 21:51
https://doi.org/10.1186/s42408-025-00394-z

Fire Ecology

RESEARCH

Open Access

Understanding drivers and dynamics of potential heat release in wet sclerophyll forests

Wey Yao Wong[1*], Jane G. Cawson[2], Thomas J. Duff[3], Patrick N. J. Lane[1] and Gary J. Sheridan[1]

Abstract

Background Potential heat release (PHR) is the theoretical maximum amount of heat releasable by wildland fuels during fire and is a key determinant of fireline intensity. Understanding its variability and dynamics is important for predicting fire behavior and effects on ecosystems. In this study, we sought to understand PHR and its drivers at the forest-stand scale. We quantified PHR for stands of wet sclerophyll forest in south-eastern Australia from field measurements of fine fuel loads, fuel moisture content, and calorific values for each fuel type. We determined the effects of species composition and live-to-dead ratio on stand-level PHR by integrating forest composition data from another study in the same forest type.

Results PHR varied from 19.8 to 77.6 MJ m^{-2} between the sites surveyed. Large differences in PHR between forest stands were primarily due to substantial differences in fuel loads and the calorific values of eucalypt versus non-eucalypt litter. Litter and canopy fuels were the primary contributors to stand-level PHR (~ 40% and ~ 30% respectively) at sites dominated by Mountain Ash (*Eucalyptus regnans* F.Muell.). In contrast, understory fuels and litter were the main contributors to PHR at the scrub site, which had no Mountain Ash. Variations in species composition between forest stands had a negligible effect on stand-level PHR compared to variations in fuel load and live-to-dead ratio.

Conclusions The significant variability in PHR could have implications for predicting fireline intensity across the landscape. Although canopy fuels are a major contributor to stand-level PHR in Mountain Ash forest, their contribution to actual heat release during a fire will depend on fire reaching the canopy via ladder fuels. Thus, forest structure and species composition may play a key role in heat release through aspects of fire behavior affecting the completeness of combustion. Further quantification of fuel consumption and live-and-dead fuel loads across the landscape is warranted for accurate determination of actual heat release during wildfire.

Keywords Fuel, Fuel moisture content, Heat yield, Wildfire, Energy release, Wet eucalypt forest, Fireline intensity

Resumen

Antecedentes La liberación del calor potencial (PHR) es la cantidad máxima teórica de calor que pueden liberar los combustibles vegetales durante un incendio, y es una determinante de la intensidad de línea. El entendimiento de variabilidad y dinámica es importante para predecir el comportamiento del fuego y sus efectos en los ecosistemas. En este estudio buscamos comprender el PHR y sus conducentes a escala de rodal forestal. Cuantificamos PHR para rodales esclerófilos húmedos en el sudeste de Australia en base a mediciones de campo de cargas de combustible

*Correspondence:
Wey Yao Wong
weyw@student.unimelb.edu.au
Full list of author information is available at the end of the article

© The Author(s) 2025. **Open Access** This article is licensed under a Creative Commons Attribution 4.0 International License, which permits use, sharing, adaptation, distribution and reproduction in any medium or format, as long as you give appropriate credit to the original author(s) and the source, provide a link to the Creative Commons licence, and indicate if changes were made. The images or other third party material in this article are included in the article's Creative Commons licence, unless indicated otherwise in a credit line to the material. If material is not included in the article's Creative Commons licence and your intended use is not permitted by statutory regulation or exceeds the permitted use, you will need to obtain permission directly from the copyright holder. To view a copy of this licence, visit http://creativecommons.org/licenses/by/4.0/.

fino, contenido de humedad, y valor calorífico de cada tipo de combustible. Determinamos los efectos de la composición de especies y la relación de vivo a muerto y el PHR a nivel de rodal mediante la integración de datos de composición del bosque de otro estudio en el mismo tipo de bosque.

Resultados El PHR varió de 19,8 a 77,6 MJ m^{-2} entre los sitios relevados. Grandes diferencias en PHR entre los rodales fueron primariamente debidas a diferencias substanciales en las cargas de combustible y el valor calorífico del mantillo de eucalipto versus el de no eucalipto. El mantillo y los combustibles del dosel fueron los principales contribuyentes del PHR a nivel de rodal (~40% y ~30%, respectivamente) en sitios dominados por eleucalipto regnans (*Eucalyptus regnans* F. Muell.). En contraste, los combustibles del sotobosque y el mantillo fueron los principales contribuyentes al PHR en los sitios de arbustales donde no se encontraba el eucalipto regnans. La variación en la composición de especies entre rodales forestales tuvo un efecto insignificante en el PHR a nivel de rodal comparado con las variaciones en la carga de combustible y en la relación vivo y el muerto (*live-to-dead ratio*).

Conclusiones La variabilidad significativa en el PHR puede tener implicancias para la predicción de la intensidad de línea a través del paisaje. Aunque los combustibles del dosel fueron los mayores contribuyentes del PHR a nivel del rodal en bosques de eucalipto regnans, su contribución a la liberación real del calor durante un incendio dependerá que el fuego llegue al dosel vía escaleras de combustible. Esto significa que la estructura y composición de la vegetación pueden jugar un rol clave en la liberación del calor a través de aspectos del comportamiento del fuego que afecten a la combustión completa. Una cuantificación a futuro del consumo de los combustibles y las cargas de combustibles vivos y muertos a lo largo de paisajes es requerido para una correcta determinación del calor liberado durante un incendio.

Background

Wildfires are a natural process of ecosystem renewal in many forests worldwide (Woodell et al. 1976; Bond and Keeley 2005). However, they can also have devastating consequences for people, ecosystems, and property. As such, understanding fire behavior is critical for mitigating the risks and impacts of wildfires.

Fire intensity refers to the amount of energy released during the combustion of organic matter and is often linked to both ecological effects of and societal impacts of wildfire (Keeley 2009). A widely used metric of fire intensity is Byram's fireline intensity (Byram 1959), which quantifies the rate of heat release per unit length of fire front. Fireline intensity is calculated using the heat yield of fuels (kJ kg^{-1}), the mass of fuel burnt or fuel load (kg m^{-2}), and the rate of spread (m s^{-1}) of the fire (Eq. 1).

$$Fireline\ intensity(\mathrm{kW m^{-1}}) = Heat_yield \times Fuel_load \times Rate_of_Spread \quad (1)$$

The heat yield and fuel load terms describe the amount of heat released from fuels when burnt. Potential heat release (PHR) is the theoretical maximum amount of heat that could be released if all fuel were consumed and is calculated from an approximation of heat yield (low heat of combustion or net calorific value) and fuel load.

Understanding how PHRs vary across the landscape is important for accurately predicting fire behavior. Fires in locations with high PHR (hence higher fireline intensities) pose a greater risk to people and infrastructure and will be more difficult to suppress (Alexander 2000; Penney et al. 2019). PHR and fireline intensity may also affect flame heights, which in turn affect the extent and severity of fire effects on vegetation (Reinhardt et al. 2001; O'Brien et al. 2018). It is important to understand how biophysical factors (e.g., stand structure, species composition, fire history, topographic position) lead to differences in PHR across the landscape, as this will help land managers predict where the risks are greater. This would assist government agencies in wildfire mitigation, response, and recovery (Opie et al. 2023). Aside from predicting wildfire risk, knowing how heat yields and fuel loads (i.e., PHR) vary across the landscape is also important for modeling fire effects on atmospheric conditions (Bakhshaii and Johnson 2019), including the development of pyroconvective clouds (Ma et al. 2023). Despite its importance, the variability and dynamics of PHR at the stand scale is poorly understood.

Calculations of PHR and fireline intensity seldom account for variability in fuel heat yields are seldom accounted for, and instead use fixed values. Many operational fire behavior models use a fixed heat yield value between 18 and 18.7 MJ kg^{-1} for calculating fireline intensity (van Wagner et al. 1992; Kenny et al. 2024). However, large differences in the heat yield of co-occurring species have also been observed (Cawson et al. 2023), with the highest heat yield values being almost 4 times that of the lowest. Heat yields of live and dead fuels may also differ due to their moisture contents. Within the same forest, the moisture content of live fuels may be an order of magnitude greater than that of dead fuels (Cawson and Duff 2019). Moisture in fuels needs energy to be evaporated during combustion (Byram 1959), and water vapor dilutes the pyrolysates making it more difficult to

generate a flammable mixture (Janssens 2005; McAllister et al. 2012). This reduces the possible amount of heat that could be released by a fuel during its combustion (i.e., its heat yield), making fuel moisture content a key determinant of heat yields and PHR.

Fuel load is another key determinant of PHR. In context of PHR and fireline intensity, fuel load refers to fine fuels, as they tend to be fully consumed in the intense fires that occur in wet sclerophyll forest (Cruz et al. 2012). Fine fuels typically comprise of dead components up to 6 mm in thickness and live components up to 3 mm in thickness including foliage (Hines et al. 2010; Keane 2015). For estimating fireline intensity, fire behavior models have used fuel accumulation models (Kenny et al. 2024), standard fuel loads for a given ecosystem type (Andrews 2018), or fuel loads estimated from visual surveys (Hines et al. 2010). A wide range of fuel load estimation models are available that have yet to be used with fire behavior models for predicting fireline intensity, and these range from the various modifications of the Olsen litter accumulation model (Olson 1963; Fox et al. 1979), to biophysical models (Duff et al. 2013; Jenkins et al. 2020), and remote sensing (Chen et al. 2017).

However, estimation of fuel loads seldom differentiate between live and dead fuels. Calculations of PHR (and fireline intensity) using these models therefore do not separately account for live and dead fuels (Leonard et al. 2023), let alone for species which have variable heat yields. This could be due the apparent dominance of dead surface fuels as the primary driver of fire spread, or the assumption that live fuels simply behave like very wet dead fuels (Finney et al. 2013). Alternatively, the lack of distinction between live and dead fuels may be due to uncertainty about the role of live fuel moisture content on flammability in forests where they are abundant (Cawson et al. 2020). Understanding the contribution of species and live-and-dead fuels heat yields towards the total chemical energy and moisture budgets of forest stands is needed to assess if the use of individual heat yield values in stand-level calculations of PHR is warranted.

Similarly, the relative importance of species composition and live-and-dead proportion on stand-PHR is unclear. Although there is a reasonably good understanding of the differences in moisture content (and heat yield) between live and dead fuels, differences between species tend to be highly location-specific and less researched. Understory species from wetter forest are reported to have lower energy content than understory species from drier forest (Dickinson and Kirkpatrick 1985), and in combination with higher moisture contents, are likely to have a lower heat yield than xeric species. However, species communities do not always fall into discrete groups across the landscape (Duff et al. 2014), so stand-level heat yields may be dependent on the species that are present at one point. Certain species may also be highly dominant where present, making up a significant proportion of fuel load locally (e.g., chamise (*Adenostoma fasciculatum* Hook. & Arn.) in California (Regelbrugge and Conard 2002)). It is unclear how much the relative abundances of live and dead fuels, as well as species composition, affect stand-level PHR.

PHR may also vary vertically between forest strata within a stand, which could have implications for fire behavior. For example, the structure, composition of load of surface fuels on the forest floor differs from understory and crown fuels and thus the PHR generated from each stratum will differ. In fire models where fuel strata are sequentially added (Kenny et al. 2024), knowledge of the vertical distribution of PHR may help to more accurately quantify changes in fire intensity for fires involving different fuel strata and the likelihood that flames will reach the next stratum, (van Wagner et al. 1992). However, the vertical distribution of fuels and their PHR has been poorly quantified in structurally complex forests with highly heterogeneous fuels (Hiers et al. 2009).

PHR is a key part of fireline intensity calculations and is important for predicting fire behavior and effects. However, the variability and drivers of its constituent components have yet to be understood. In this study, we sought to quantify PHR at the stand scale by measuring fuel moisture content, heat yields, and fuel loads. We used case study sites in wet sclerophyll forest in Victoria, Australia, as they have abundant live fuels (Cruz et al. 2018), large seasonal shifts in fuel moisture content (Brown et al. 2022b), and stark differences in stand structure for different successional stages (Brown et al. 2021).

Specifically, we asked:

1. What is the contribution of individual fuel types to stand-level moisture and PHR in wet sclerophyll forest?
2. How is PHR distributed vertically in wet forest stands with contrasting fire histories?
3. Are species composition and live fuel proportion important drivers of differences in PHR between forest stands?

Methods

We quantified PHR for three contrasting wet sclerophyll forest stands by measuring fuel load and structure for the dominant species, their calorific value and moisture content (Table 2). We combined these data with stand

structure measurements to understand how PHR is vertically distributed. We then used a regression model to estimate fuel loads from species cover abundance data from a prior study (Ashwell 1985) that consisted of a larger range of wet sclerophyll forest communities. Using the modeled fuel loads, we calculated PHR for these forest communities to examine the influence of species composition and live fuel proportion on stand-level PHR.

Study site description

The study occurred in two case study locations comprising wet sclerophyll forest in central-eastern Victoria, Australia. The first location was in Yarra State Forest, approximately 70 km east of Melbourne, Australia (Fig. 1). The second location was in Sherbrooke Forest Park, 35 km east of Melbourne. Both locations were similar in their climate, soils, and vegetation, with mild wet winters and warm dry summers (climate type Cfb (Peel et al. 2007)). Across both locations, mean maximum and minimum temperatures ranged from around 25 °C in January to 3 °C in July respectively, with mean annual rainfall between 1000 and 1500 mm (BoM 2025). Both had deep soils which were high in organic matter and topped with abundant litter.

The vegetation at both case study areas is broadly classified as wet sclerophyll forest and was dominated by Mountain Ash (*Eucalyptus regnans* F.Muell.), which formed a tall open canopy. Mountain Ash is an obligate seeder species, regenerating in single aged stands from seeds released during infrequent but intense fires (Ashton 1981). Repeat fires over a short interval may cause localized extinction of Mountain Ash if the trees are burned before reaching reproductive age (Bowman et al. 2014). The understory beneath the Mountain Ash was structurally diverse, consisting of subdominant ferns, shrubs, and grasses (Tables 1 and 2). The structure and composition of wet sclerophyll forests is strongly related to stand age and fire history, with distinct communities and successional stages having been well documented (Ashton 2000; Fairman et al. 2015; Bowd et al. 2023).

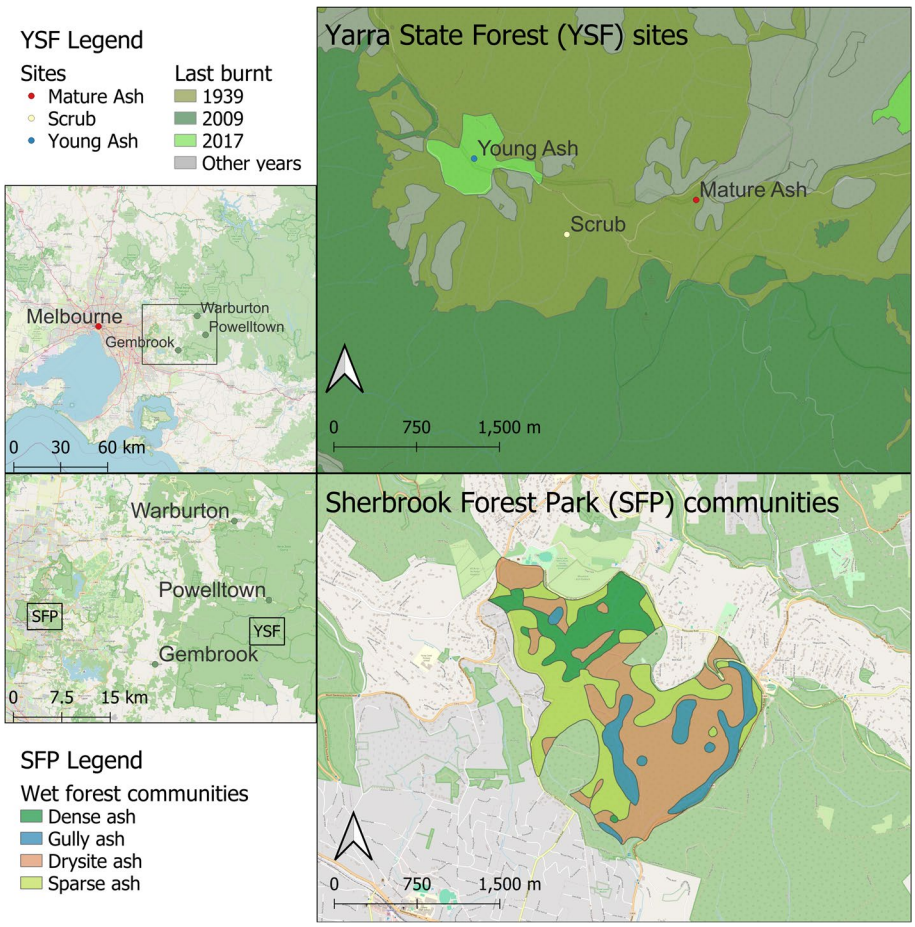


Fig. 1 Location of case study sites. Yarra State Forest (YSF) with fuel load sampling sites; map shows fire history of surrounding area. Sherbrooke Forest Park (SFP) showing location of each wet forest community within the reserve

At the Yarra State Forest, we measured fuel load, fuel moisture, and calorific values at three sites previously used in Burton et al. (2019) and Brown et al. (2021): Young Ash, Mature Ash, and scrub (Table 2 and Fig. 1). These sites are examples of wet sclerophyll forest with different fire histories and thus vast differences in understory compositions (Table 2). The Young Ash site was burnt in 2017 after being logged and is taken to be representative of the structure and composition of a newly regenerating (6 years post-fire) Mountain Ash-dominated forest. Both the Mature Ash and scrub sites were burnt in 1939. The Mature Ash site is taken to be representative of the structure and composition of a mature Mountain Ash-dominated forest stand. The scrub site had experienced two close succession fires 1926 and 1932 before being burnt again in 1939, leading to localized extirpation of the Mountain Ash. Instead, the scrub site is dominated by mesic species (ferns and shrubs) typical of the understory in Mountain Ash forests. The structure of all three sites have previously been characterized using LiDAR in Brown et al. (2021) and Brown (2022). Each site had more than 12 replicate plots, which were determined using stratified random points allocated in GIS. They derived mean canopy heights and light penetration index at 0.5 m for each replicate plot and compared it against the values derived for each site. When these replicate values were plotted against site values, all mean replicate values were within 1 standard deviation of the 1:1 line. This demonstrated that the structure of the sites was indeed representative and typical of forests with the same fire histories, or "forest state."

The second case study location was in Sherbrooke Forest Park. These sites were all dominated by Mountain Ash in the overstory, but exhibited a range of understory compositions (Table 2), reflecting different fire histories and topographic positions. Data for this location was collected as part of a prior study by Ashwell (1985) to identify key factors influencing species composition in Mountain Ash forests. He conducted 289 vegetation surveys, recording dominant species and their projective foliage cover. His survey methodology was similar to the non-destructive survey methodology we used for the Yarra State Forest sites, described in the next subsection. Through his analysis, Ashwell (1985) identified distinct vegetation communities of wet sclerophyll forest, which we use as additional examples of wet sclerophyll forest stands with differing compositions and structures. Here we refer to Ashwell's sites in order of increasing stand age as sparse Ash, dense Ash, dry site Ash, and (moist) gully Ash. A summary of main understory species is provided (Table 2).

Table 1 Plant species included in this study and their grouping by growth form

Growth form	Species Latin name	Common name
Tree	*Acacia dealbata* Link	Silver wattle
	Acacia melanoxylon R.Br	Blackwood
	Eucalyptus regnans F.Muell	Mountain Ash
	Persoonia arborea F.Muell	Tree geebung
Shrub	*Correa lawrenceana* Hook	Mountain correa
	Hedycarya angustifolia A.Cunn	Austral mulberry
	Olearia argophylla (Labill.) Benth	Musk daisy-bush
	Pomaderris aspera Sieber ex DC	Hazel pomaderris
	Prostanthera melissifolia F.Muell	Balm mint-bush
Fern	*Blechnum wattsii* Tindale	Hard water-fern
	Dicksonia antarctica Labill	Soft tree-fern
	Polystichum proliferum (R.Br.) C.Presl	Mother shield-fern
Graminoids	*Gahnia sieberiana* Kunth	Red-fruit saw-sedge
	Tetrarrhena juncea R.Br	Forest wiregrass

Fuel load estimation

For the Yarra State Forest sites, we determined live and dead fine fuel loads with a combination of destructive sampling and visual surveys. The same person did both the destructive sampling and the surveys to ensure consistency. We estimated fuel loads at the Sherbrooke Forest Park communities with a regression model using cover abundance.

Destructive sampling

We undertook destructive sampling in temporary plots adjacent (< 50 m) to the permanent 10 × 10 m plots in the Yarra State Forest to avoid disturbing the fuels and forest structure. Litter fuels were the exception and were sampled from within the permanent plots. We did not sample species with cover < 5% as their contribution to potential heat release was considered insubstantial relative to the dominant species.

For litter fuels, we collected samples from three random points within each permanent plot (site coordinates in Table 2) that were fully covered by litter (no bare soil or rock). We measured the mean litter depth with a ruler and disk at each point to estimate bulk density, then cut out < 6 mm diameter litter from a 0.04 m^2 microquadrat at each point. The collected litter samples were weighed in the field to the nearest 0.1 g using an A&D EJ-1500 Precision Compact Lab Balance, and recorded their dry weight after oven-drying at 105 °C for 2 weeks.

To determine the fuel loads of bark, we collected 8–12 strips of suspended bark ribbons with different lengths and widths (0.6–2 m length and 2–5 cm width) from within the vicinity of each of the Ash sites (< 50 m). We then used their measured dimensions to determine the

Table 2 Case study forest areas and site (or community) characteristics. Attributes are for specific sites in the Yarra State Forest and average attributes per community for Sherbrooke Forest Park. As there were numerous subdominant understory species, we listed those with >20% cover. Ash = Mountain Ash = *Eucalyptus regnans*

Location	Forest type	Stand age	Site coordinates	Elevation (m)	Slope (°)	Aspect	Canopy species	Main understory species (% cover)	Source
Yarra State Forest (YSF)	Young Ash	6 (burnt 2017)	−37°54′1.75″ 145°43′56.30″	735	5	158	*Eucalyptus regnans* *Acacia dealbata*	*Tetrarrhena juncea* (35%)	This study
	Mature Ash	84 (burnt 1939)	−37°54′11.73″ 145°45′18.76″	725	13	160	*Eucalyptus regnans*	*Dicksonia antarctica* (60%)	
	Scrub (Collapsed Ash)	84 (burnt 1939)	−37°54′24.39″ 145°44′30.86″	635	15	167	*Acacia dealbata* *Persoonia arborea*	*Blechnum wattsii* (20%) *Dicksonia antarctica* (20%)	
Sherbrooke Forest Park (SFP)	Sparse Ash (Community 3.1)	27–62 (as of 1985)	n/a—37 sites within SFP	432 (mean)	8 (mean)	33 (median)	*Eucalyptus regnans*	*Tetrarrhena juncea* (25%) *Olearia argophylla* (26%)	Ashwell 1985
	Dense Ash (Community 4.1)	62 (as of 1985)	n/a—52 sites within SFP	410 (mean)	10 (mean)	34 (median)	*Eucalyptus regnans*	*Tetrarrhena juncea* (69%)	
	Dry site Ash (Community 2.4)	62–180 (as of 1985)	n/a—23 sites within SFP	409 (mean)	16 (mean)	30 (median)	*Eucalyptus regnans*	*Pomaderris aspera* (27%) *Polystichum proliferum* (29%) *Tetrarrhena juncea* (31%)	
	Moist gully Ash (Community 1.1)	180–300 (as of 1985)	n/a—13 sites within SFP	357 (mean)	16 (mean)	31 (median)	*Eucalyptus regnans*	*Dicksonia antarctica* (67%) *Acacia melanoxylon* (21%) *Polystichum proliferum* (20%)	

average mass of 1 cm^2 of bark, which was found to be 0.019 g cm^{-2} or 1.9×10^{-8} t per cm^2. This value was used as the calibration value for estimating the fuel load of bark strips during the visual surveys.

Due to the diversity of understory plants, we used different sampling methodologies for each growth form (shrub, fern, graminoid). In general, we conducted destructive sampling on individual plants, harvesting a portion or segments (shoots, fronds) to determine their fine fuel loads in relation to the number of segments sampled.

The sampling methodology for shrubs was based on the "Adelaide method" (Andrew et al. 1979), where a segment of a shrub or a "representative shoot" was harvested. A representative shoot for shrubs at the sites generally consisted of a branch 30–40 cm long, which consisted of 10–20% of the entire individual shrub. From the representative shoot, we collected all fine fuel (i.e., live foliage and stem segments < 3 mm in diameter), discarding the coarser material, then oven-dried and weighed the collected fine fuel. We sampled representative shoots from 8 to 12 plants of each species to estimate the average fine fuel load of representative shoots of a given species, which was used as the calibration value for the visual survey.

We used a similar approach for determining the fine fuel loads on the fronds of fern species. We harvested mature whole fronds, collected live foliage and stem

segments < 3 mm in diameter and discarding the coarser material. We harvested fronds from 8 to 12 plants, then measured the oven-dry weight of the stripped off foliage and stems. We did not sample more than one frond from tree-ferns as their mature fronds did not appear to vary significantly. The average oven-dry weight of fronds was used as the calibration value for estimating fern species fuel load.

We determined fuel loads for graminoid species using double sampling with regression (Catchpole 1987), which was suitable for large single species patches (Catchpole and Wheeler 1992). Common graminoids in wet sclerophyll forest such as forest wiregrass tend to follow this growth pattern (Fogarty 1993). We cut out a 1 m^2 quadrat of the graminoid, ensuring that no other plant species or fuel was harvested. We removed fallen debris from the harvested sample, but did not remove dead attached portions of the dead graminoid. We also discarded stems that were > 3 mm where necessary. We harvested eight patches of each graminoid species, then oven-dried and weighed the harvested material. The average oven-dry weight of the harvested material was determined as a calibration value for estimating graminoid species fuel loads during the visual surveys (Table 3).

Visual surveys

We conducted visual surveys on 19th February 2023 within the permanent plots, centered on preexisting weather stations. The plots were squares measuring 10 × 10 m (100 m^2), which were large enough to assess biomass and carbon in biomass estimation studies (Specht and West 2003).

We measured an additional 12 points of litter depth from random litter covered points in each plot and estimated the total litter cover across the plot. We calculated total litter fuel load in the plot by multiplying the average bulk density (g cm^{-3}) of the collected litter samples, litter depth (cm), plot:microquadrat area, and litter cover (%) (Eq. 2).

$$FL_{litter}\,(\mathrm{t/ha}) = bulk\ density \times litter\ depth \times \frac{100}{0.04} \times cover \tag{2}$$

We counted fallen bark ribbons where possible and estimated the number of bark ribbons attached to trees, and estimated their average lengths and widths. We calculated bark fuel loads by multiplying the bark calibration value by their lengths (cm) and widths (cm), and number of ribbons (Eq. 3). We also determined elevated fuel loads by adding the estimated dead proportions of other live fuel groups (Eq. 4).

$$FL_{bark}\,(\mathrm{t/ha}) = length_{ribbons} \times widths_{ribbons} \times 1.9 \times 10^{-8} \times number_{ribbons} \tag{3}$$

Table 3 Fuel heat yields and mean fuel moisture content (FMC) for late summer (19th February 2023) and winter (9th August 2023). Heat yield values are reproduced from Wong et al. (2025) with permission. Superscript letters indicate that the energy content was obtained from the literature, and heat yield calculated from sampled FMC

Fuel type	Group	State	Heat yield (MJ kg^{-1})	Summer FMC (%)	Winter FMC (%)
Bark or aerial dead fuels	Bark	Dead	18.73	32.60	42.98
Mountain Ash litter	Litter	Dead	16.81	20.66	233.98
Scrub litter	Litter	Dead	12.84	24.13	270.68
Hard water-fern	Fern	Live	10.27	257.61	286.27
Soft tree-fern	Fern	Live	13.29	185.55	239.25
Mother shield-fern	Fern	Live	12.18	224.74	239.84
Forest wiregrass	Graminoid	Live	10.21	276.45	287.20
Red-fruit saw-sedge	Graminoid	Live	16.93	80.30	120.42
Mountain correa	Shrub	Live	11.42	260.65	196.20
Austral mulberry	Shrub	Live	10.14	450.51	361.50
Musk daisy-bush	Shrub	Live	13.43	235.64	194.36
Hazel pomaderris	Shrub	Live	14.48	182.64	219.60
Balm mint-bush	Shrub	Live	14.24	158.86	255.85
Silver wattle	Tree	Live	16.21[a]	173.45	183.64
Mountain Ash	Tree	Live	18.14[b]	139.05	159.76
Tree geebung	Tree	Live	13.66[c]	220.19	253.43

[a] Nunes et al. (2020)

[b] Frederick et al. (1985)

[c] Mean energy content from tree group used

$$FL_{elevated_dead}(\text{t/ha}) = FL_{bark} + FL_{dead\ parts\ of\ other\ fuels} \quad (4)$$

We did not destructively sample canopy fuels due to site constraints and also because many allometric models are available in the literature for estimating tree biomass. We measured the top height of trees using a rangefinder where possible (except Mountain Ash), measured their diameter at breast height (DBH) with a tape measure, and their cover abundance. We used existing LiDAR data from Brown et al. (2021) to determine the height of tall Mountain Ash. To estimate tree biomass, we used an allometric model from Bi et al. (2004) to estimate foliage mass in kg, which was assumed to be the fine fuel load (Eq. 5, where n = number of trees in the plot). For Mountain Ash, we used foliage mass from the literature matching with the ages of stands surveyed (Frederick et al. 1985; Sillett et al. 2015), multiplied by its stocking density (Ashton 1976) as its fine fuel load. Total canopy fuel load was determined to be the estimated fuel load of the Mountain Ash plus the foliage mass calculated from the allometric equation multiplied by 0.1 for the conversion to t^{-1} ha (Eq. 6).

$$FL_{trees}(\text{kg}) = \sum_{t=1}^{n_{trees}} \exp(-2.393 + 1.303\ln(DBH_t)) \times (100 - \%dead) \quad (5)$$

$$FL_{canopy}(\text{t/ha}) = 0.1 \times (FL_{trees}(\text{kg}) + FL_{mountain\ ash}(\text{kg})) \quad (6)$$

For each individual shrub, we counted the number of representative shoots on an individual. The fuel load for a given shrub was calculated by multiplying the previously determined calibration value (weight of the representative shoot (in kg)) multiplied by the number of shoots, and the site total for a given shrub species was the sum of all constituent individuals multiplied by 0.1 for the conversion to t ha^{-1} (Eq. 7). We also recorded the cover abundance of each species (all individuals of a species) within each plot, as well as their average height by species.

$$FL_{shrubs}(\text{t/ha}) = 0.1 \times \sum_{s=1}^{n_{shrubs}} weight_{rep_shoot} \times n_{shoots} \times (100 - \%dead) \quad (7)$$

Similarly, we measured fine fuel loads of ferns by counting the number of fronds of each species within the plot. We also recorded the average height of each fern species. We calculated fuel loads by multiplying the previously determined calibration value (weight of fronds) by the number of fronds for each species, multiplying by 0.1 to convert to t ha^{-1} (Eq. 8).

$$FL_{ferns}(\text{t/ha}) = 0.1 \times \sum_{f=1}^{n_{ferns}} weight_{frond} \times n_{fronds} \times (100 - \%dead) \quad (8)$$

Graminoid fuel loads were estimated using the estimated area covered within the plot. We estimated the coverage of each graminoid species in m^2 within the plot and multiplied this by the calibration value (previously determined weight of 1 m^2), multiplied by 0.1 (Eq. 9). We also determined cover abundance by dividing cover abundance of the graminoid species by the plot area and recorded their average height.

$$FL_{graminoids}(\text{t/ha}) = 0.1 \times \sum_{g=1}^{n} weight_{patch} \times cover_{patch} \times (100 - \%dead) \quad (9)$$

Regression model

We used the species fuel loads calculated from the visual surveys and their cover abundance to generate a regression for estimating fuel loads from cover for each plant growth form (trees, shrubs, ferns, grasses). Their terms are shown (Table 4), and the equation is in the form of Eq. 10. This regression was used to predict fuel load by growth form from the Ashwell (1985) cover abundance data. This allowed us to include a broader range of sites in the forest composition analysis.

$$Fuel\ load = \exp(a \times cover + c) \quad (10)$$

Estimating fuel loads from Sherbrooke Forest Park

For the Sherbrooke Forest sites, we used the species data from the Ashwell (1985) study and predicted fuel loads using their reported cover abundance metric. In Ashwell (1985), the authors used cover index as the cover metric, which represented the "average cover" of the species across the multiple sites comprising the community. As this value peaked at 87.5, we divided the reported cover indexes of each species by 87.5 then multiplied by 100 to approximate cover abundance (which scales from 0% to 100%). Then, we estimated fuel loads of each live fuel species using the log-linear model for its growth form that relates cover abundance to fuel load (Eq. 10, Table 4).

As the quantity of dead fuels was not recorded in the Ashwell study, we estimated the average proportion of dead fuel to estimate its abundance. At the

Table 4 Log-linear models for estimating fuel loads from cover abundance and their coefficients. The cover abundance and fuel loads were determined from the Yarra State Forest sites. The equations take the form of Eq. 10

	n	*a*	*c*	R^2
Tree	5	0.1017	−1.4587	0.9792
Shrub	7	0.1104	−2.1208	0.6943
Fern	6	0.0298	−0.8262	0.247
Graminoid	2	0.0342	−0.7394	NA

Yarra State Forest sites, live fuel proportion was around 40%. Therefore, we estimated the dead fuel loads at the Sherbrooke Forest Park communities to be 1.5 times (60%dead:40%live) the live fuel loads, with the total fuel loads being the sum of live and dead fuels. To assess the effect of live fuel proportion on site PHR, we scaled the live fuel load as a proportion of the previously calculated total fuel load, keeping all the relative proportions of species equal.

Determination of fuel moisture

Fuel moisture content was determined gravimetrically for live and dead fine fuels. Sampling occurred in late summer (19th February 2023) and in winter (9th August 2023), and fuels were collected between 12 noon and 3 pm local time to capture the driest daytime conditions. For live fuels, each species with a cover abundance of more than 5% was sampled individually. We followed protocol 19 from Yebra et al. (2024) for sampling live fuel moisture, where we collected at least 30 g of shoots < 3 mm including stems and live foliage. Samples were collected from three individual plants per species and aggregated into the same bag. For dead fuels, we followed Slijepcevic et al. (2018) for sampling dead fuel moisture. We sampled bark ribbons suspended at around 1.5 m on understory foliage and from where they have mostly detached from trees. We also sampled surface and subsurface litter on the forest floor < 6 mm in diameter from at least 3 points within the 10 × 10 m permanent plot. We calculated mean litter fuel moisture content by scaling surface and subsurface litter moisture content according to their relative depths. Like in the visual survey, we considered surface litter to be the top 1 cm of the litter layer and subsurface litter starting from 1 cm down to mineral soil. We weighed all fresh samples (live and dead) in the field using an A&D EJ-1500 Precision Compact Lab Balance and transported them in double bagged Ziploc bags. We dried the samples at 105 °C for a week (Matthews 2010), or until the mass of the samples stopped reducing.

Determination of energy content and heat yield

The samples collected for fuel moisture determination in late summer were subsequently used for determining energy content. We determined heat yields in Wong et al. (2025) and used a subset of the data (late summer heat yields) to calculate PHR in this study. Samples were ground using a Retsch Ultra Centrifugal Mill ZM200 with a 1.0 mm filter. Then, we used oxygen bomb calorimetry to determine the gross calorific value for each fuel type (species or dead fuel strata), following the ISO 1716 standard with a CAL3K Bomb Calorimeter. We ran samples in duplicate, with approximately 0.3 g of powdered sample per replicate, and report here the average for each fuel type. We loaded samples into gelatine capsules to avoid the dispersion of loose powder during ignition in the bomb calorimeter, adjusting the final gross calorific value (GCV) reading for the mass and calorific value of the gelatine capsule (Atwater and Snell 1903). We determined the hydrogen composition (H_d) using the same powdered samples, using the Thermo Scientific FlashSmart CHNS analyzer, then calculated heat yield using Eq. 11.

$$Heat\ yield = GCV - 0.02442(9H_d + \%FMC) \quad (11)$$

Data analysis

To determine the contribution of individual fuel types to stand-level energy and moisture (research question 1) at our Yarra State Forest sites, we calculated fine fuel moisture storage and PHR for each fuel type. We multiplied fuel loads (t ha^{-1}), fuel moisture content (%), and a unit conversion factor of 0.001 to determine water storage of each fuel in mm for summer and winter. To determine PHR, we multiplied fuel loads (in kg m^2) by heat yields (MJ kg^{-1}) for PHR in MJ m^2. We then summed individual species moisture storage and PHR by their growth form.

To understand the vertical distribution of PHR (research question 2), we plotted PHR of individual species against their average heights, but grouped (colored) species by fuel type. This enabled us to quantify the vertical distribution of PHR in greater detail than existing fuel load models that collapse fuels into strata (surface, near-surface, elevated, canopy). We then compared this against existing LiDAR data of the point cloud profiles and percentage return profiles of similar forests assessed in Brown et al. (2021).

To determine whether species composition and live fuel proportion are important drivers of PHR (research question 3), we calculated PHR for each forest community identified in Sherbrooke Forest Park. We used these communities as an extension to the wet sclerophyll forest case study at the Yarra State Forest. We used the same method for calculating PHR as for the Yarra State Forest sites, although several assumptions had to be made to estimate PHR for species whose heat yields were not known. For species whose heat yields were not measured, we used gross calorific values from the literature. To calculate heat yield from the acquired gross calorific values, we assumed their moisture content was the mean fuel moisture content measured for the vegetation group, following Eq. 11. We also assumed that the hydrogen content was 5.747%, which corresponds to 1.263 MJ kg^{-1} of latent heat absorbed for the vaporization of the water of reaction for woody fuels (Byram 1959; Alexander 1982).

We conducted data analysis using R statistical software (version 4.3.3) (R Core Team 2021). We aggregated individual species values (by summing) into species groups when calculating fuel loads, water storage, and PHR. We produced all graphs using the ggplot package (Wickham 2016), with some using patchwork (Pederson 2025) and viridis (Garnier et al. 2023).

Results

Total energy and moisture storage in fuels

Heat yields were highly variable between co-occurring species sampled (Table 3), ranging from 18.73 MJ kg^{-1} for bark fuels to 10.27 MJ kg^{-1} for forest wiregrass (*Tetrarrhena juncea*). Overall, fuel moisture was lower in summer than in winter. The fuel moisture content of litter increased by more than tenfold (20.66% to 233.98%) from summer to winter, while changes in the fuel moisture content of bark and live fuels increased or changed by no more than half. Litter from the scrub site had a substantially lower gross calorific value (15.55 MJ kg^{-1}) than litter from the Ash sites (16.81 MJ kg^{-1}), reflecting the lower gross calorific values of the dominant species (ferns at the scrub site vs. eucalypt litter at the Ash sites). The site mean heat yield value were 19.8 MJ kg^{-1} for the Young Ash site, 20.3 MJ kg^{-1} for the Mature Ash site, and 15.8 MJ kg^{-1} for the scrub site.

Though fireline intensity is calculated with fuel loads in kg m^2 (1 kg m^2 = 10 t ha^{-1}), here we present fuel loads in t ha^{-1} for ease of comparison with other fuel load studies. Fuel load was also differed substantially between the sites, with the Mature Ash site having the highest fuel load (42.55 t ha^{-1}), followed by the Young Ash (28.05 t ha^{-1}), then the scrub (16.04 t ha^{-1}) (Fig. 2a). The litter bed and the Mountain Ash canopy were the largest components of the fuel load at the Young Ash and Mature Ash sites (11.0–17.0 t ha^{-1} and 6.9–17.0 t ha^{-1} respectively), followed by aerial dead fuels (Fig. 2a). There were also substantial differences between the aerial dead fuel load between sites, with the Young Ash site having 6.75 t ha^{-1} compared to the Mature Ash site (5.40 t ha^{-1}). Live understory fuels made up the smallest proportion of site fuel load in the Mature Ash (~7%) but had a higher relative abundance in the Young Ash and scrub sites, which had less dominant canopies. Given the relatively small contribution of individual understory species, we aggregated all species by their growth form (tree, shrub, graminoid, fern). All sites had higher dead fuel loads than live fuels, with the Young Ash having the highest proportion of dead fuels at 58%, and the scrub having the lowest (48%). Most of the dead fuel was litter on the forest floor across all sites, as opposed to aerial dead fuel.

There were substantial differences in PHR between each site, with the Mature Ash site having the highest PHR at 77.6 MJ m^{-2}, followed by Young Ash (48.7 MJ m^{-2}) and scrub (19.8 MJ m^{-2}) (Fig. 2b). The largest sources of PHR in the Ash sites were the litter and the canopy fuels, making up 41–43% and 25–37% respectively. Understory contribution to PHR was only around 7–8% for the Ash sites, but made up more of site PHR for scrub (35%).

There was also a substantial difference in water storage between sites, with the Mature Ash site having the greatest amount of water storage (4.06 mm), followed by the Young Ash (2.23 mm) and scrub (2.04 mm) over summer (Fig. 2c). Across all sites, dead fuel moisture storage made up about a quarter of water storage for all sites in summer and about half in winter (Fig. 2d). Live fuel moisture storage had a larger increase from winter to summer for the Ash sites (+30% approx.) than the scrub site (+8%). Despite the relatively small shifts in moisture content of the dominant Mountain Ash canopy between summer and winter, its abundance amplified small changes in fuel moisture content.

Vertical distribution of PHR and site structure

There were large variations in forest stand structure between the case study sites, and while the litter and Mountain Ash canopies were the largest sources of PHR, there was a large gap between them (Fig. 3a). In the Ash stands, there was sparse foliage along most of the tree trunks (Fig. 3b), with most of the foliage being well elevated from the understory vegetation (~12 m separation in the Young Ash, ~28 m in the Mature Ash). On the other hand, all fuels were within 0.5 m vertically of other fuels at the scrub site. However, the exact vertical distribution of bark fuels at the Ash sites were not recorded, so the size of the vertical gaps between the canopy and elevated fuels or understory vegetation could not be exactly quantified.

Site composition scenarios

PHR varied significantly across all forest compositions (24 to 99 MJ m^{-2}), assuming all sites had 40% live fuel (note that PHR from YSF sites may differ between Figs. 2 and 4 as their fuel loads were scaled to a fixed 40% live fuels for ease of comparison in Fig. 4). Total site fine fuel load was by far the most important determinant of stand-level PHR; changes in its quantity resulted in a direct and proportional change in site PHR. For comparison, the sparse Ash and the dry Ash sites had similar understory compositions, with only the canopy and dead fuels differing substantially in fuel load (+9.5 t ha^{-1} and +17.6 t ha^{-1} respectively). In total, their site fuel loads differed by 27.1 t ha^{-1}, and at 40% live proportion, their PHR differed by about 48 MJ m^{-2}.

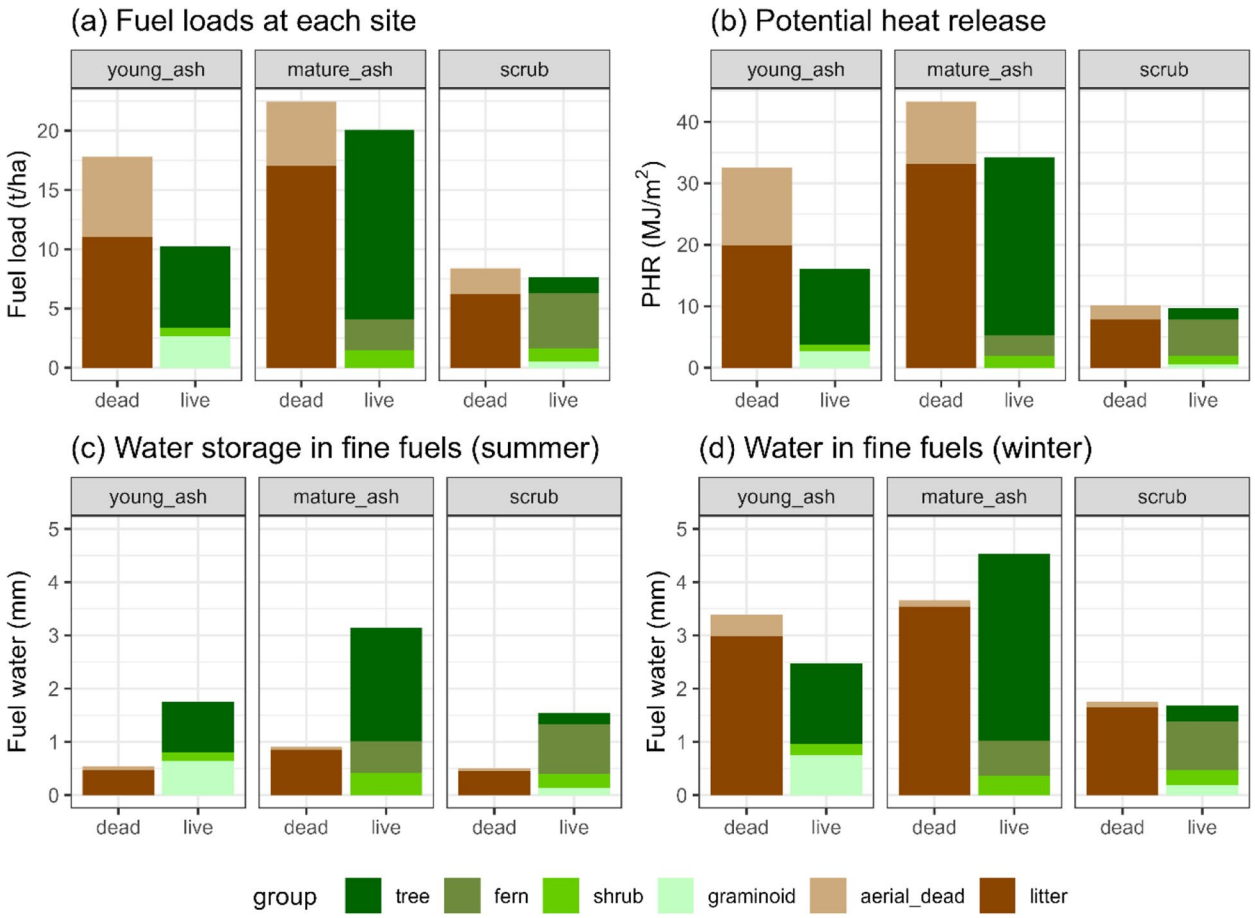


Fig. 2 **a** Fuel loads at each site, **b** potential heat release by fuel group, **c** total fine fuel moisture storage in summer, and **d** total fine fuel moisture storage in winter. Aerial dead fuels consist of bark and elevated or near-surface dead fine fuels. All values were calculated by species and aggregated in plot by fuel group

The proportion of live fuels at a site was of lesser importance than fuel load on PHR. A 10% reduction in live fuel load resulted in around a 5% increase in PHR. Dramatic declines in live fuel load from 70% to 10% only resulted in increases of 9–21% PHR for each site.

Species composition also appeared to be of less importance to PHR than fuel load. This is demonstrated by comparing the gully Ash and Young Ash sites, which had similar total fuel loads and live proportions, but differed substantially in their species composition. The Young Ash was dominated by Mountain Ash, while the gully Ash was dominated by ferns with a significantly lower heat content than the Mountain Ash (Table 3). Despite these vast differences in species composition, at the same level of live fuel proportion the stand-level PHR only differed by 0–8% between the sites.

Discussion

Litter and canopy fuels dominate forest PHR

Litter fuels and canopy fuels had the highest fuel loads, and corresponding total energy content and PHR was high. These results align with existing understanding of eucalypt forest fuel loads, with surface fuels (litter) being the most abundant fuel type, and canopy fuels being the next most abundant (Nguyen et al. 2024). The large vertical gaps observed in our study between understory and overstory fuels in the mature forest stand also align with previous studies of fire risk in tall eucalypt forest (Furlaud et al. 2021). The canopy trees of mature forests are tall (sometimes reaching more than 70 m) and thus much taller than the dominant height of the understory, which is less than 10 m. The litter and canopies of the eucalypt trees also contributed most to the total PHR in a forest stand, given the high calorific value of eucalypt leaves compared with other forest fuels (Dickinson and Kirkpatrick 1985; Cawson et al. 2023).

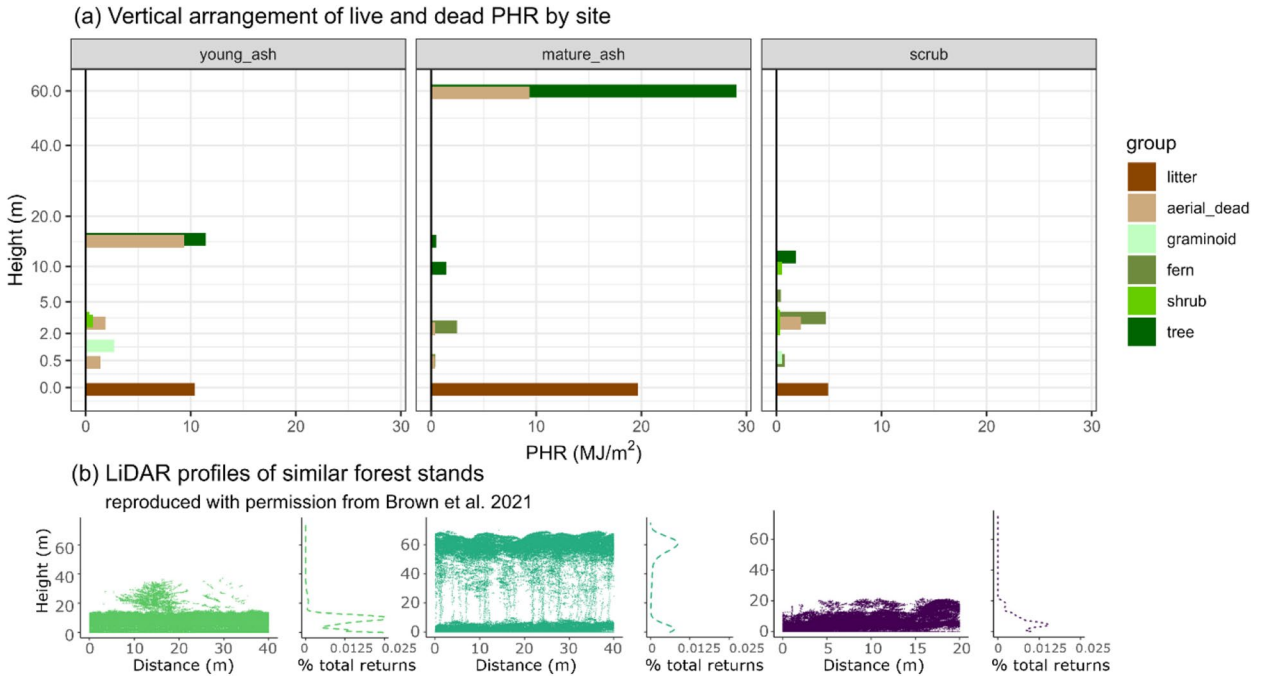


Fig. 3 **a** Vertical distribution of summer potential heat release at each site with exponential height axis. Heights of each fuel in the barplots reflect its average height with the exception of canopy being top height. Heights do not indicate that the entire fuel load of the given individual or species is concentrated at that given height (i.e., tree stratum is distributed vertically). The height of bark fuels is represented by the height of the canopy, as their exact distribution across the vertical stratum could not be recorded. **b** Point cloud profiles and percentage return profiles from Brown et al. (2021) of forest stands with similar fire histories within Yarra State Forest, reproduced with permission

Our observation of litter fuel as a key contributor to stand-level PHR aligns with others who identify litter as the primary driver of fire spread (Finney et al. 2013). Surface fuel (litter) consumption contributes significantly to fire behavior in Australian models (Cruz et al. 2015), and its heat release during fire subsequently affects whether the fire reaches the canopy (van Wagner 1977). The high PHR of the canopy in the forest stands means that there would be a substantial increase in fire intensity when fire shifts from being a surface fire to a canopy fire (crowning). The consumption of canopy fuels depends on the intensity of the surface fire, as well as the vertical connectivity of fuels (Ritter et al. 2023). Large gaps between the understory and canopy fuels in Mountain Ash stands may be overcome if there are large amounts of bark to act as "ladder fuels" (Sullivan et al. 2012), or given sufficiently strong understory winds (Alexander and Cruz 2011). Quantification of the vertical distribution of bark and other ladder fuels remains difficult due to their comparatively lower fuel loads and patchy distribution, but warrants further research given their importance in the consumption of canopy fuels.

More than just live and dead: a need to account for overstory, understory, and dead fuel moisture

Fuel moisture content differed substantially between live and dead fuels, with dead fuels showing more than a tenfold increase in fuel moisture between summer and winter, while live fuels were more stable. The fuel moisture content of canopy fuels was more stable than understory live fuels but caused larger fluctuations in overall site moisture storage due to their abundance, which amplified small changes in fuel moisture. On the other hand, overall moisture storage in the live understory fuels showed minimal change when aggregated by plant group, likely because opposing trends among individual species offset each other.

Differences in fuel moisture between canopy and understory live fuels aligned with our expectations of their moisture dynamics. Numerous studies have observed greater variability in shrubs compared to co-occurring tree species (Viegas et al. 2001; Pellizzaro et al. 2007; Nolan et al. 2018), and it is thought that the deeper roots of trees enable them to access deeper moisture stores (Resco De Dios 2020) and therefore be less sensitive to fluctuations in landscape dryness. However, the fuel moisture content of some species sampled were higher in summer than in winter. A possible explanation

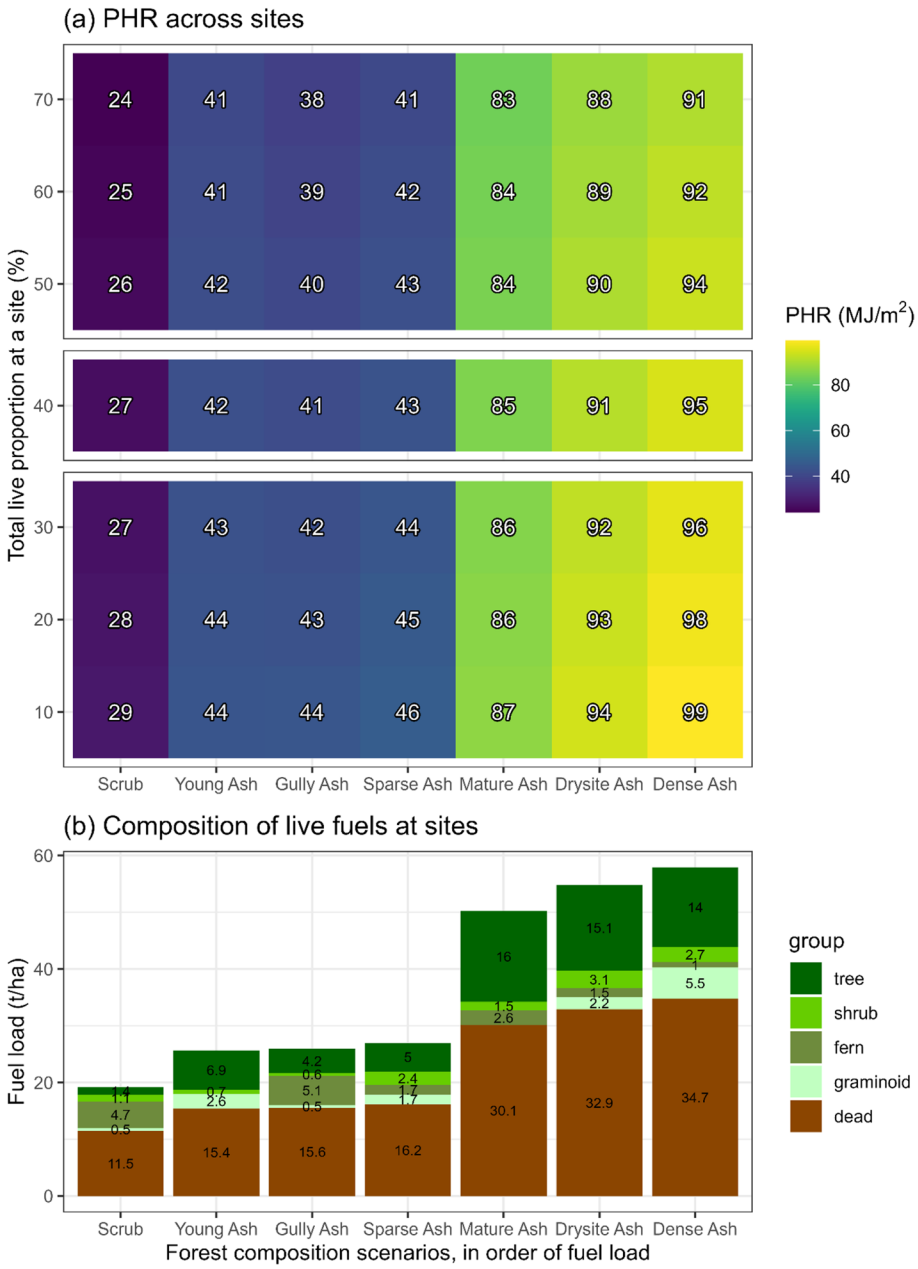


Fig. 4 **a** Potential heat release for each site, with site on x-axis and varying live fuel proportions on the y-axis. Forty percent was estimated as the average live fuel proportion across these sites, corresponding to fuel loads in **b**, hence the other PHR above and below 40% represent changes to live fuel proportion. **b** Total (predicted) fuel loads at sites showing makeup of different fuel components, with the live proportion at each site set at exactly 40% to enable clearer comparisons

for the observed discrepancy is that the understory vegetation was not under water stress during summer, as the region received record rainfall leading up to the 2022–2023 summer season. In the months of August, October, and November, rainfall exceeded the 90th percentile for the region (BoM 2025). In the absence of water stress, species fuel moisture content may have been driven by changes in dry matter (chemical changes in foliage), which has been observed in conifers (Brown et al. 2022a) but was not measured in our study.

The dissimilarities of understory and canopy moisture dynamics highlights the need to account for them separately in models of live fuel moisture content. Differences in fuel moisture content between the understory and

overstory may not be observed by remote sensing, as they only provide an aggregate moisture content (Danson and Bowyer 2004; Qi et al. 2012; Fan et al. 2018). More recent models have successfully predicted fuel moisture content for individual species (Balaguer-Romano et al. 2022), which may assist with exploring the differences in the dynamics of fine fuel moisture in forest stands.

The significant differences in fuel moisture content between live and dead fuels translated into differences in their heat yields, which is used to calculate PHR. Current fire behavior models tend to use a constant value of around 18.6 MJ kg^{-1}, overestimating the heat yields of understory species by 40–50% due to their high fuel moisture content. In mature Mountain Ash forests, this overestimation may have minimal impact on fire intensity calculations, as understory fuels make up a relatively small proportion of the total fuel load. In contrast, in areas without a Mountain Ash overstory—such as the scrub site—understory species dominate the fuel load, making this overestimation much more consequential for modeling fire intensity accurately. Given the projected increase in fire occurrence under climate change (Keenan and Nitschke 2016), repeated fires may lead to an expansion of forest areas resembling the scrub site (Brown 2022). As a result, future predictions of fireline intensities for these altered landscapes may need to account for the lower heat yields of fuels in wet sclerophyll forests lacking a Mountain Ash overstory.

Fuel load is the most important determinant of PHR, followed by live proportion, then species composition

Total fuel loads had the largest influence on PHR compared to live proportion and species composition. Each percent of fuel load increase corresponded approximately to a percent increase in PHR, while each percent decrease in live fuel proportion corresponded to approximately half a percent increase in PHR. Meanwhile, the largest difference in species composition only resulted in about 3–10% difference in PHR between drastically different sites.

The small effect of species composition on PHR is unsurprising, given the large influence of the litter bed and canopy on PHR. The heat yields measured in this study showed that understory live fuels had generally lower heat yields than the canopy fuels, so any effect of species composition on PHR is likely associated with variations in the dominance of the canopy. These results suggest that the effect of variations in species composition will be negligible to PHR of the forest stand during an intense fire where all fine fuels are completely consumed, such as those in wet eucalypt forest. For this forest type, it is likely unnecessary to consider the species composition in studies of large-scale heat release, such as in atmospheric instability and pyro-cumulonimbus formation. However, species composition may play a more significant role in other forests, such as those with greater vegetation dynamics and seasonality in species composition. Further research should also assess the importance of species composition on PHR in other forest types.

PHR only represents energy in Byram's (1959) fireline intensity equation (Eq. 1), leaving the rate term (rate of spread) still to be accounted for. This term may be sensitive to fuel or species attributes, so the contribution of individual species to fireline intensity is not merely from its heat release. Individual plants vary in their flammability as a function of their physical structure and traits (Schwilk 2015; Cawson et al. 2023), and the dominance of certain species in a forest stand may substantially alter its flammability. For example, forest wiregrass had very low heat yields and did not make up a substantial part of the forest fuel mass. However, it is known to substantially increase the flammability of forest stands due to its fine structure, scrambling habit, and ability to catch fallen litter, which enables it to burn exceptionally quickly and easily (Fogarty 1993). Therefore, PHR only represents the upper limit of energy that may be released in a given forest stand. Other factors such as fuel structure (bulk density, surface area) and moisture affect how much of it is actually released during fire.

Actual heat release during wildfire is dependent on other factors and fire severity not a reliable indicator

In this study, we used the heat yield and fine fuel load terms in Byram's fireline intensity to calculate PHR, assuming all fine fuels were completely consumed. Our range of PHR values (24 to 99 MJ m^2), multiplied by a known rate of spread for a given fire, seemed to match well with their reported fireline intensity results that assumed heat yields were 18.6 MJ kg^{-1}. We multiplied our PHR values with the average rate of spread (90 m min^{-1} or 1.5 m s^{-1}) reported in a similar forest type from the 2009 Kilmore East fire (Cruz et al. 2012). This produced fireline intensities of between 36,000 and 148,500 kW m^{-1}, which were similar to the average fireline intensity of 82,677 kW m^{-1} reported in that study for a similar forest type.

However, our methodology for estimating fuel loads may not accurately represent the fuels that are actually consumed during fire. Another study assessing post-fire fuel loads in the same 2009 fire found that fuels up to 7.5 cm diameter were completely consumed, while consumption for larger fuels ranged from 80 to 100% (Hollis et al. 2011). Therefore, a substantial proportion of heat release during the 2009 fire may have come from coarse fuels, which were not captured in this study. On the other

hand, less intense fires may consume only a small proportion of fine live fuels (Nolan et al. 2022). More research into the drivers and extent of fuel consumption across all size classes is needed to better reflect actual stand-scale heat release.

Additionally, other factors contributing to the consumption of fuels should also be considered. The ability of flames to reach the fuels, to heat fuels to ignition temperatures, and the adequacy of heat release to heat other fuels to continue the reaction are all important considerations for actual heat release during a fire. Likewise, the conditions during a wildfire differ from the conditions within a calorimeter when the heat contents of fuels are sampled under pressurized oxygen. Recent studies have sought to improve the method for quantifying heat released from fuel samples burnt in air (Madrigal et al. 2011; Melnik et al. 2022), which show significantly lower values compared to those taken with a bomb calorimeter. Further research combining the flammability of fuels and their consumption under field conditions is needed to provide a better understanding of the actual heat release from forest stands during wildfires.

Post-fire severity mapping is sometimes used as a measure of forest fire intensity (Hammill and Bradstock 2006), with crown fires and subsequent canopy consumption often assumed to represent the most intense fires. The results from this study highlights that not all crown fires are comparable in terms of heat release. A crown fire in a mature wet sclerophyll forest would likely release far more energy than a crown fire in a young forest due to having a higher canopy fuel load and therefore PHR. In contrast, transitioning from a surface to a crown fire in the scrub site would have a far smaller impact on heat release as the crown was a small contributor to PHR. That said, fires are less likely to burn the canopy in mature forests as there is a larger vertical gap between the understory and the canopy fuel strata.

Limitations

Apart from the incomplete consumption of fuel, other heat losses may also reduce actual heat release. Byram (1959) recognized that radiative losses could comprise a substantial proportion (10–20%) of fuel heat yields. Although difficult to measure, van Wagner (1972) argues that accounting for radiant losses is important as it likely has a significant effect on fire behavior, and so should be included. Another heat loss not accounted for in this study is the heat of desorption, which is the energy needed to separate bound water from wood. At approximately 116.3 kJ kg^{-1} according to Byram (1959), this value is one or two order of magnitudes smaller than the other sources of heat losses from vaporization of fuel moisture and water of reaction. Its negligible amount is highly unlikely to affect results as they are currently presented.

There were large variations in PHR between the three sites considered in this study. As these sites were within 2 km of each other, their large differences in PHR suggests that PHR may vary significantly across the landscape between forest stands with alternative structures and compositions. Future research should focus on accurate quantification of fuel loads as the main drivers of PHR. A greater number of stand-level PHR measurements will be useful for estimating its variability across the landscape. Other wet sclerophyll forest states should also be included, such as the *Acacia*-dominated scrubs in places where the Mountain Ash has failed to regenerate (Bowd et al. 2023), as they may become more prevalent across the landscape due to changing fire regimes.

Conclusions

We calculated PHR in a range of wet sclerophyll forest case study sites through measuring fuel loads, energy content, and fuel moisture content of fuels. There were substantial differences in PHR across the sites, primarily due to differences in site fuel load. Fuel loads were dominated by litter and canopy fuels across the Ash sites, but understory fuels were more significant in the scrub site. There were large differences in the moisture of live and dead fuels, as well as between understory and canopy fuels, highlighting the need to separately account for them in PHR.

While canopy fuels made up a large part of PHR in sites dominated by Mountain Ash, their considerable height would likely make it difficult for fires to reach and burn them. The ability of fires to spread to and consume canopy fuels in part depends on ladder fuels, which may vary substantially between forest stands. Thus, forest structure and species composition—though not major drivers of PHR—may play a key role in heat release by affecting of fire behavior and the completeness of combustion of canopy fuels.

Current approaches may be overestimating wildfire heat release through assuming a constant value of heat yield and complete combustion of the fuel load. At the same time, they may underestimate heat release by assuming complete combustion of only fine fuels. Accurate determination of actual heat release for estimating fireline intensity should therefore focus on the extent of fuel consumption of each fuel type and size class. A greater number of measurements of PHR across the landscape is needed to quantify its variability, focusing on accurate quantification of fuel loads as its major driver.

Abbreviation

PHR Potential heat release

Acknowledgements
The authors acknowledge T. Mwamulima for assistance with fieldwork. This research was conducted on Wurundjeri and Bunurong land, and the authors pay our respect to their Elders past and present. Finally, we also thank the two anonymous reviewers for their detailed comments and suggestions for the manuscript.

Authors' contributions
WW conceptualized the project, collected and analysed data, and wrote the manuscript. JC, PL, TD, and GS provided supervision and intellectual input. All authors were involved in reviewing and editing of the final manuscript.

Funding
This research was funded by an Australian Government Research Training Program (RTP) scholarship, as well as the Integrated Forest Ecosystem Research (IFER) program, which is a joint research agreement between the University of Melbourne and the Victorian Department of Energy, Environment and Climate Action.

Data availability
The data used in this study will be shared upon reasonable request to the corresponding author.

Declarations

Ethics approval and consent to participate
Not applicable.

Consent for publication
Not applicable.

Competing interests
The authors declare no competing interests.

Author details
[1]School of Agriculture, Food and Ecosystem Sciences, Faculty of Science, The University of Melbourne, Biosciences 1 (Building 123), Parkville, VIC 3010, Australia. [2]School of Agriculture, Food and Ecosystem Sciences, Faculty of Science, The University of Melbourne, Burnley Campus, 500 Yarra Boulevard, Richmond, VIC 3121, Australia. [3]Country Fire Authority, 8 Lakeside Dr, Burwood East, VIC 3151, Australia.

Received: 30 April 2025 Accepted: 24 July 2025
Published online: 02 September 2025

References

Alexander, M. E. 1982. Calculating and interpreting forest fire intensities. *Canadian Journal of Botany* 60:349–357. https://doi.org/10.1139/b82-267.

Alexander, ME. 2000. Fire behaviour as a factor in forest and rural fire suppression. Forest Research Bulletin (No. 197, 5). iv + 28 pp. Available at https://www.ruralfireresearch.co.nz/__data/assets/pdf_file/0009/63945/31037-FireBehaviourSuppression.pdf.

Alexander, M. E., and M. G. Cruz. 2011. Interdependencies between flame length and fireline intensity in predicting crown fire initiation and crown scorch height. *International Journal of Wildland Fire* 21:95–113. https://doi.org/10.1071/WF11001.

Andrew, M.H., I.R. Noble, and R.T. Lange. 1979. A non-destructive method for estimating the weight of forage on shrubs. *The Rangeland Journal* 1: 225. https://doi.org/10.1071/RJ9790225.

Andrews, P. L. 2018. The Rothermel surface fire spread model and associated developments: A comprehensive explanation. *USDA for Serv - Gen Tech Rep RMRS-GTR* 2018:1–121.

Ashton, D.H. 1976. The development of even-aged stands of *Eucalyptus regnans* F. Muell. in Central Victoria. *Australian Journal of Botany* 24: 397–414.

Ashton, DH. 1981. Fire in tall open forests (wet sclerophyll forests). In 'Fire and the Australian Biota'. (Eds AM Gill, RH Groves, IR Noble) pp. 339–366. The Australian Academy of Science: Canberra, ACT.

Ashton, D. H. 2000. The big ash forest, Wallaby Creek, Victoria—changes during one lifetime. *Australian Journal of Botany* 48:1. https://doi.org/10.1071/bt98045.

Ashwell D. 1985. The importance of Tetrarrhena juncea R.Br. in the ecology of Eucalyptus regnans stands in Sherbrooke Forest Park. Dissertation, University of Melbourne.

Atwater, W.O., and J.F. Snell. 1903. Description of a bomb-calorimeter and method of its use. *Journal of the American Chemical Society* 25: 659–699. https://doi.org/10.1021/ja02009a001.

Bakhshaii, A., and E. A. Johnson. 2019. A review of a new generation of wildfire–atmosphere modeling. *Canadian Journal of Forest Research* 49:565–574. https://doi.org/10.1139/cjfr-2018-0138.

Balaguer-Romano, R., R. Díaz-Sierra, M. De Cáceres, et al. 2022. A semi-mechanistic model for predicting daily variations in species-level live fuel moisture content. *Agricultural and Forest Meteorology* 323 : 109022. https://doi.org/10.1016/j.agrformet.2022.109022.

Bi, H., Turner, J., Lambert, Marcia, J. 2004. Additive biomass equations for native eucalypt forest trees of temperate Australia. Trees 18:. https://doi.org/10.1007/s00468-004-0333-z.

BoM. 2025. Bureau of Meteorology Climate Data Online. Available at http://www.bom.gov.au/jsp/ncc/cdio/weatherData/av?p_nccObsCode=139&p_display_type=dataFile&p_startYear=&p_c=&p_stn_num=086094. Accessed 12 Dec 2024.

Bond, W.J., and J.E. Keeley. 2005. Fire as a global 'herbivore': The ecology and evolution of flammable ecosystems. *Trends in Ecology & Evolution* 20: 387–394. https://doi.org/10.1016/J.TREE.2005.04.025.

Bowd, E. J., L. McBurney, and D. B. Lindenmayer. 2023. The characteristics of regeneration failure and their potential to shift wet temperate forests into alternate stable states. *For Ecol Manag* 529 : 120673. https://doi.org/10.1016/j.foreco.2022.120673.

Bowman, D.M.J.S., B.P. Murphy, D.L.J. Neyland, et al. 2014. Abrupt fire regime change may cause landscape-wide loss of mature obligate seeder forests. *Global Change Biology* 20: 1008–1015. https://doi.org/10.1111/gcb.12433.

Brown, T. P., Hoylman, Z. H., Conrad, E., Holden, Z., Jencso, K., Jolly, W. M. 2022. Decoupling between soil moisture and biomass drives seasonal variations in live fuel moisture across co-occurring plant functional types. *Fire Ecology* 18(1):14. https://doi.org/10.1186/s42408-022-00136-5.

Brown, T. P., A. Inbar, T. J. Duff, et al. 2021. Forest structure drives fuel moisture response across alternative forest states. *Fire* 4 : 030048. https://doi.org/10.3390/fire4030048.

Brown, T. P., Z. H. Hoylman, E. Conrad, et al. 2022a. Decoupling between soil moisture and biomass drives seasonal variations in live fuel moisture across co-occurring plant functional types. *Fire Ecology*. https://doi.org/10.1186/s42408-022-00136-5.

Brown, T. P., A. Inbar, T. J. Duff, et al. 2022b. The sensitivity of fuel moisture to forest structure effects on microclimate. *Agricultural and Forest Meteorology* 316 : 108857. https://doi.org/10.1016/j.agrformet.2022.108857.

Burton, J.E., J. Cawson, P. Noske, and G. Sheridan. 2019. Shifting states, altered fates: Divergent fuel moisture responses after high frequency wildfire in an obligate seeder eucalypt forest. *Forests* 10: 1–16. https://doi.org/10.3390/f10050436.

Byram, G.M. 1959. Combustion of forest fuels. In Forest fire: Control and use. Ed. KP Davis, 61–89. New York: McGraw-Hill.

Catchpole, W. R. 1987. Heathland fuel and fire modelling. Dissertation, UNSW Sydney.

Catchpole, W. R., and C. J. Wheeler. 1992. Estimating plant biomass: A review of techniques. *Australian Journal of Ecology* 17:121–131. https://doi.org/10.1111/j.1442-9993.1992.tb00790.x.

Cawson, J.G., and T.J. Duff. 2019. Forest fuel bed ignitability under marginal fire weather conditions in Eucalyptus forests. *International Journal of Wildland Fire* 28: 198–204. https://doi.org/10.1071/WF18070.

Cawson, J. G., V. Hemming, A. Ackland, et al. 2020. Exploring the key drivers of forest flammability in wet eucalypt forests using expert-derived conceptual models. *Landscape Ecology* 35:1775–1798. https://doi.org/10.1007/s10980-020-01055-z.

Cawson, J. G., J. E. Burton, B. J. Pickering, et al. 2023. Quantifying the flammability of living plants at the branch scale: Which metrics to use? *International Journal of Wildland Fire*. https://doi.org/10.1071/WF23007.

Chen, Y., X. Zhu, M. Yebra, et al. 2017. Development of a predictive model for estimating forest surface fuel load in Australian eucalypt forests with

LiDAR data. *Environmental Modelling & Software*. https://doi.org/10.1016/j.envsoft.2017.07.007.
Cruz, M.G., A.L. Sullivan, J.S. Gould, et al. 2012. Anatomy of a catastrophic wildfire: The Black Saturday Kilmore East fire in Victoria, Australia. *Forest Ecology and Management* 284: 269–285. https://doi.org/10.1016/j.foreco.2012.02.035.
Cruz, M. G., Gould, J. S., Alexander, M. E., Sullivan, A. L., McCaw, W. L., Matthews, S. 2015. A guide to rate of fire spread models for Australian vegetation. Australasian Fire and Emergency Service Authorities Council Limited and Commonwealth Scientific and Industrial Research Organisation.
Cruz, M. G., J. S. Gould, J. J. Hollis, and W. L. McCaw. 2018. A hierarchical classification of wildland fire fuels for Australian vegetation types. *Fire (Basel)* 1:1–39. https://doi.org/10.3390/fire1010013.
Danson, F. M., and P. Bowyer. 2004. Estimating live fuel moisture content from remotely sensed reflectance. *Remote Sensing of Environment* 92:309–321. https://doi.org/10.1016/j.rse.2004.03.017.
Dickinson, K. J. M., and J. B. Kirkpatrick. 1985. The flammability and energy content of some important plant species and fuel components in the forests of Southeastern Tasmania. *Source J Biogeogr* 12:121–134.
Duff, T. J., T. L. Bell, and A. York. 2013. Predicting continuous variation in forest fuel load using biophysical models: A case study in south-eastern Australia. *International Journal of Wildland Fire* 22:318–332. https://doi.org/10.1071/WF11087.
Duff, T. J., T. L. Bell, and A. York. 2014. Recognising fuzzy vegetation pattern: The spatial prediction of floristically defined fuzzy communities using species distribution modelling methods. *Journal of Vegetation Science* 25:323–337. https://doi.org/10.1111/jvs.12092.
Fairman, T. A., C. R. Nitschke, and L. T. Bennett. 2015. Too much, too soon? A review of the effects of increasing wildfire frequency on tree mortality and regeneration in temperate eucalypt forests. *International Journal of Wildland Fire* 25:831–848. https://doi.org/10.1071/WF15010.
Fan, L., J.-P. Wigneron, Q. Xiao, et al. 2018. Evaluation of microwave remote sensing for monitoring live fuel moisture content in the Mediterranean region. *Remote Sensing of Environment* 205:210–223. https://doi.org/10.1016/j.rse.2017.11.020.
Finney, M. A., J. D. Cohen, S. S. McAllister, and W. M. Jolly. 2013. On the need for a theory of wildland fire spread. *International Journal of Wildland Fire* 22:25–36. https://doi.org/10.1071/WF11117.
Fogarty, L. G. 1993. The accumulation and structural development of the wiregrass (Tetrarrhena juncea) fuel type in East Gippsland. Fire Management Branch, Department of Conservation and Natural Resources: Vic, Australia.
Fox, B. J., M. D. Fox, and G. M. Mckay. 1979. Litter accumulation after fire in a eucalypt forest. *Australian Journal of Botany* 27:157–165.
Frederick, D. J., H. A. I. Madgwick, M. F. Jurgensen, and G. R. Oliver. 1985. Dry matter content and nutrient distribution in an age series of *Eucalyptus regnans* plantations in New Zealand. *New Zealand Journal of Forestry Science* 15:158–179.
Furlaud, J.M., L.D. Prior, G.J. Williamson, and D.M.J.S. Bowman. 2021. Fire risk and severity decline with stand development in Tasmanian giant *Eucalyptus* forest. *For Ecol Manag* 502: 119724. https://doi.org/10.1016/j.foreco.2021.119724.
Garnier, S., Ross, N., BoB, Rudis., Filipovic-Pierucci, A., Galili, T., Timelyportfolio, O'Callaghan A., Greenwell, B., Sievert, C., Harris, D.J., Sciaini, M., JJ, Chen. 2023. viridis(Lite) - Colorblind-Friendly Color Maps for R. (Zenodo). https://doi.org/10.5281/ZENODO.4679423
Hammill, K. A., and R. A. Bradstock. 2006. Remote sensing of fire severity in the Blue Mountains: Influence of vegetation type and inferring fire intensity. *International Journal of Wildland Fire* 15:213–226. https://doi.org/10.1071/WF05051.
Hiers, J. K., J. J. O'Brien, R. J. Mitchell, et al. 2009. The wildland fuel cell concept: An approach to characterize fine-scale variation in fuels and fire in frequently burned longleaf pine forests. *International Journal of Wildland Fire* 18:315–325. https://doi.org/10.1071/WF08084.
Hines, F., Tolhurst, K. G., Wilson, A. A., McCarthy, G. J. 2010. Overall fuel hazard assessment guide. Fire Management Branch, Dept of Natural Resources and Environment.
Hollis, J.J., S. Matthews, W.R. Anderson, et al. 2011. Behind the flaming zone: Predicting woody fuel consumption in eucalypt forest fires in southern Australia. *Forest Ecology and Management* 261: 2049–2067. https://doi.org/10.1016/J.FORECO.2011.02.031.
Janssens, M. L. 2005. Chapter 10 - material flammability. In Handbook of environmental degradation of materials, ed. M. Kutz, 207–225. Norwich, NY: William Andrew Publishing.
Jenkins, M. E., M. Bedward, O. Price, and R. A. Bradstock. 2020. Modelling bushfire fuel hazard using biophysical parameters. *Forests* 11:925. https://doi.org/10.3390/f11090925.
Keane, R.E. 2015. *Wildland fuel fundamentals and applications*. Cham: Springer International Publishing.
Keeley, J. E. 2009. Fire intensity, fire severity and burn severity: A brief review and suggested usage. *International Journal of Wildland Fire* 18:116–126. https://doi.org/10.1071/WF07049.
Keenan, R. J., and C. Nitschke. 2016. Forest management options for adaptation to climate change: A case study of tall, wet eucalypt forests in Victoria's Central Highlands region. *Australian Forestry* 79:96–107. https://doi.org/10.1080/00049158.2015.1130095.
Kenny, B. J., S. Matthews, S. Sauvage, et al. 2024. Australian fire danger rating system: Implementing fire behaviour calculations to forecast fire danger in a research prototype†. *International Journal of Wildland Fire* 33:NULL-NULL. https://doi.org/10.1071/WF23142.
Leonard, J., Arena, A., Opie, K., et al. 2023. National Bushfire Intelligence Capability (NBIC) Stage 1 collection. 397.50 GB.
Ma, W., C. S. Wilson, J. J. Sharples, and Z. Jovanoski. 2023. Investigating the effect of fuel moisture and atmospheric instability on pyrocb occurrence over southeast Australia. *Atmosphere* 14:1087.
Madrigal, J., M. Guijarro, C. Hernando, et al. 2011. Effective heat of combustion for flaming combustion of Mediterranean forest fuels. *Fire Technology* 47: 461–474. https://doi.org/10.1007/s10694-010-0165-x.
Matthews, S. 2010. Effect of drying temperature on fuel moisture content measurements. *International Journal of Wildland Fire* 19:800–802. https://doi.org/10.1071/WF08188.
McAllister, S., I. Grenfell, A. Hadlow, et al. 2012. Piloted ignition of live forest fuels. *Fire Safety Journal* 51:133–142. https://doi.org/10.1016/j.firesaf.2012.04.001.
Melnik, O. M., S. A. Paskaluk, M. Y. Ackerman, et al. 2022. New in-flame flammability testing method applied to monitor seasonal changes in live fuel. *Fire (Basel)* 5:1–29. https://doi.org/10.3390/fire5010001.
Nguyen, T.H., S. Jones, K.J. Reinke, and M. Soto-Berelov. 2024. Estimating fine fuel loads in eucalypt forests using forest inventory data and a modelling approach. *For Ecol Manag* 561: 121851. https://doi.org/10.1016/j.foreco.2024.121851.
Nolan, R. H., J. Hedo, C. Arteaga, et al. 2018. Physiological drought responses improve predictions of live fuel moisture dynamics in a Mediterranean forest. *Agricultural and Forest Meteorology* 263:417–427. https://doi.org/10.1016/j.agrformet.2018.09.011.
Nolan, R.H., O.F. Price, S.A. Samson, et al. 2022. Framework for assessing live fine fuel loads and biomass consumption during fire. *Forest Ecology and Management* 504: 119830. https://doi.org/10.1016/J.FORECO.2021.119830.
Nunes, L.J.R., M.A.M. Raposo, C.I.R. Meireles, et al. 2020. Control of invasive forest species through the creation of a value chain: *Acacia dealbata* biomass recovery. *Environments* 7: 39. https://doi.org/10.3390/environments7050039.
O'Brien, J. J., J. K. Hiers, J. M. Varner, et al. 2018. Advances in mechanistic approaches to quantifying biophysical fire effects. *Current Forestry Reports* 4:161–177. https://doi.org/10.1007/s40725-018-0082-7.
Olson, J. S. 1963. Energy storage and the balance of producers and decomposers in ecological systems. *Ecology* 44:322–331. https://doi.org/10.2307/1932179.
Opie K, Arena A, Leonard J, et al (2023) Methodology for national bushfire hazard mapping - National Bushfire Intelligence Capability (NBIC) Stage 1. https://doi.org/10.25919/0H5F-2F14
Pedersen, T. 2025. patchwork: The Composer of Plots. R package version 1.3.1.9000, https://github.com/thomasp85/patchwork.
Peel, M. C., B. L. Finlayson, and T. A. McMahon. 2007. Updated world map of the Köppen-Geiger climate classification. *Hydrology and Earth System Sciences* 11:1633–1644. https://doi.org/10.5194/hess-11-1633-2007.
Pellizzaro, G., P. Duce, A. Ventura, and P. Zara. 2007. Seasonal variations of live moisture content and ignitability in shrubs of the Mediterranean basin. *International Journal of Wildland Fire* 16: 633–641. https://doi.org/10.1071/WF05088.

Penney, G., D. Habibi, M. Cattani, and M. Carter. 2019. Calculation of critical water flow rates for wildfire suppression. *Fire (Basel)* 2:1–12. https://doi.org/10.3390/fire2010003.
Qi, Y., P. E. Dennison, J. Spencer, and D. Riaño. 2012. Monitoring live fuel moisture using soil moisture and remote sensing proxies. *Fire Ecology* 8:71–87. https://doi.org/10.4996/fireecology.0803071.
R Core Team. 2021. R: a language and environment for statistical computing. R Foundation for Statistical Computing, Vienna, Austria.
Regelbrugge, J. C., Conard, S. G. 2002. Biomass and fuel characteristics of chaparral in southern California. Assoc Fire Ecol Misc Publ No 1 308–317 308–317.
Reinhardt, E. D., R. E. Keane, and J. K. Brown. 2001. Modeling fire effects. *International Journal of Wildland Fire* 10:373. https://doi.org/10.1071/WF01035.
De Resco Dios, V. 2020. *Plant-fire interactions: Applying ecophysiology to wildfire management*. Cham: Springer International Publishing.
Ritter, S. M., C. M. Hoffman, M. A. Battaglia, et al. 2023. Vertical and horizontal crown fuel continuity influences group-scale ignition and fuel consumption. *Fire* 6:321. https://doi.org/10.3390/fire6080321.
Schwilk, D. W. 2015. Dimensions of plant flammability. *New Phytologist* 206:486–488. https://doi.org/10.1111/nph.13372.
Sillett, S.C., R. Van Pelt, R.D. Kramer, et al. 2015. Biomass and growth potential of *Eucalyptus regnans* up to 100m tall. *Forest Ecology and Management* 348: 78–91. https://doi.org/10.1016/J.FORECO.2015.03.046.
Slijepcevic, A., W. R. Anderson, S. Matthews, and D. H. Anderson. 2018. An analysis of the effect of aspect and vegetation type on fine fuel moisture content in eucalypt forest. *International Journal of Wildland Fire* 27:190–202. https://doi.org/10.1071/WF17049.
Specht, A., and P. W. West. 2003. Estimation of biomass and sequestered carbon on farm forest plantations in northern New South Wales, Australia. *Biomass and Bioenergy* 25:363–379. https://doi.org/10.1016/S0961-9534(03)00050-3.
Sullivan, A. L., McCaw. W. L., Cruz, M. G., et al. 2012. Fuel, fire weather and fire behaviour in Australian ecosystems. Flammable Aust Fire Regimes Biodivers Ecosyst Chang World 51–77.
Van Wagner, C. E. 1972. Heat of combustion, heat yield, and fire behaviour. Environment Canada Forestry Service.
Van Wagner, C. E., Stocks, B. J., Lawson, B. D., et al. 1992. Development and structure of the Canadian forest fire behavior prediction system. For Can Fire Danger Group Inf Rep ST-X-3Ottawa ON.
van Wagner, C. E. 1977. Conditions for the start and spread of crown fire. *Canadian Journal of Forest Research* 7:23–34. https://doi.org/10.1139/x77-004.
Viegas, D. X., J. Piñol, M. T. Viegas, and R. Ogaya. 2001. Estimating live fine fuels moisture content using meteorologically-based indices. *International Journal of Wildland Fire* 10:223–240. https://doi.org/10.1071/wf01022.
Wickham, H. 2016. *ggplot2: Elegant graphics for data analysis*. New York: Springer-Verlag.
Wong. W. Y., Cawson, J., Duff, T., Lane, P., Sheridan, G. 2025. Understanding variability in heat yields of wet sclerophyll forest fuels. *International Journal of Wildland Fire* 34(9). https://doi.org/10.1071/WF24227.
Woodell, S. R. J., T. T. Kozlowski, and C. E. Ahlgren. 1976. *Fire and ecosystems*. Elsevier.
Yebra, M., G. Scortechini, K. Adeline, et al. 2024. Globe-LFMC 2.0, an enhanced and updated dataset for live fuel moisture content research. *Scientific Data* 11 : 332. https://doi.org/10.1038/s41597-024-03159-6.

Publisher's Note

Springer Nature remains neutral with regard to jurisdictional claims in published maps and institutional affiliations.